Renewable Energy 141 (2019) 1092–1102

Contents lists available at ScienceDirect

Renewable Energy

journal homepage: www.elsevier.com/locate/renene

# Predictable changes in fish school characteristics due to a tidal turbine support structure

Benjamin Williamson [a, b, *], Shaun Fraser [c, d], Laura Williamson [a], Vladimir Nikora [c], Beth Scott [a]

[a] School of Biological Sciences, University of Aberdeen, Aberdeen, UK
[b] Environmental Research Institute, University of the Highlands and Islands (UHI), Thurso, UK
[c] School of Engineering, University of Aberdeen, Aberdeen, UK
[d] NAFC Marine Centre, Port Arthur, Scalloway, Shetland, UK

ARTICLE INFO

*Article history:*
Received 26 October 2018
Received in revised form
3 March 2019
Accepted 14 April 2019
Available online 15 April 2019

*Keywords:*
Environmental monitoring
Environmental impact
Fish behaviour
Marine renewable energy
Tidal stream turbine

ABSTRACT

There is uncertainty on the ecological effects of tidal stream turbines. Concerns include animal collision with turbine blades, disruption of migratory and foraging behaviour, attraction of animals to prey aggregating around turbines, or conversely displacement of animals from preferred habitat.

This study used concurrent ecological and physical measurements to show the predictability of fish school characteristics (presence, school area and height above seabed) in a high energy tidal site across spring/neap, ebb/flood and daily cycles, and how this changed around a turbine structure.

The rate of schools and school area per hour increased by 1.74 and 1.75 times respectively around a turbine structure compared to observations under similar conditions without a turbine structure. The largest schools occurred at peak flow speeds and the vertical distribution of schools over the diel cycle was altered around the turbine structure.

While predictable attraction or aggregation of prey may increase prey availability and predator foraging efficiency, attraction of predators has the potential to increase animal collision risk. Predictable changes from the installation of turbine structures can be used to estimate cumulative effects on predators at a population level. This study can guide a strategic approach to the monitoring and management of turbines and arrays.



## 1. Introduction

With rapid development of marine renewable energy extraction, uncertainty surrounding the environmental and ecological effects of installing and operating tidal stream turbines remains [1]. Species at risk from impacts vary among sites, often including fish, seabirds and marine mammals. Particular focus is given to populations that are protected due to their increased vulnerability to external factors that threaten their viability [2]. Concerns include animal collision risk, disruption of migratory and foraging behaviour, attraction of animals to turbines or to prey attracted to or aggregating around turbines, or conversely displacement from preferred habitat [3]. Changes in behaviour of fish species, in particular those which are common prey of seabirds and marine mammals, could lead to changes in foraging behaviour of their predators as observed at offshore wind turbines [4].

### 1.1. Collision risk

The collision of animals (fish, diving seabirds, marine mammals) with rotating turbine blades has the potential to cause injury or mortality. Direct observation of a collision is limited by sensor capabilities [2]. Instead, efforts focus on estimating collision *risk*, i.e. the probability of an animal encountering a moving blade, for example above a nominal tidal turbine cut-in speed of 1 m/s [5], and the animal failing to evade the blade [6]. The effectiveness of collision risk modelling therefore relies on accurate empirical data on animal presence and animal distribution and behaviour in the vicinity of tidal turbines [7] rather than assuming a uniform density

* Corresponding author. Environmental Research Institute, North Highland College, University of the Highlands and Islands (UHI), Thurso, KW14 7EE, UK.
*E-mail addresses:* benjamin.williamson@uhi.ac.uk (B. Williamson), shaun.fraser@uhi.ac.uk (S. Fraser), lauradwilliamson@gmail.com (L. Williamson), v.nikora@abdn.ac.uk (V. Nikora), b.e.scott@abdn.ac.uk (B. Scott).

https://doi.org/10.1016/j.renene.2019.04.065

or distribution of animals. It is also important to consider the predictability of animal occurrence at the height of the rotor swept area across tidal and diel cycles in order to target any monitoring and potential mitigation techniques.

### 1.2. Foraging efficiency and hydrodynamics

The 'tidal-coupling hypothesis' links hydrodynamic characteristics, many of which are temporally and spatially predictable across tidal phase, to prey distribution, abundance and availability across trophic levels [8]. In areas of high tidal flow velocity, naturally-forming hydrodynamic patterns such as strong horizontal and/or vertical shear, and current velocities up to 4 m/s have the potential to aggregate, disaggregate and disorient prey, or provide a physical barrier within the water column. These hydrodynamic effects can aid predator capture of prey, increasing foraging efficiency [1,9]. Distinct spatial and temporal patterns of animal behaviour in tidal sites have been linked to hydrodynamics for seals [10] and diving seabirds [9], and changes to the distribution and behaviour of fish have been shown to be more important than changes in relative fish abundance [8].

Where the sustained flow velocity exceeds the cruising speed of fish species found in these sites [11], it is hypothesised that the tidal-coupling becomes episodic tidal-forcing as physiological limits are exceeded and fish either become advected with the flow or seek areas of lower flow velocity. Selective tidal-stream transport is used by both benthic fish and migrating pelagic fish, e.g., mackerel and herring [1].

In addition to the natural hydrodynamics of tidal sites, flow modification by tidal turbines is hypothesised to have an effect up to 2–5 rotor diameters upstream [12] and >10 rotor diameters downstream [13]. The range at which this is discernible from the background turbulent flow is highly dependent on the site hydrography and turbine design [3]. Fish may seek refuge around tidal turbine structures, either from flow [2] in the lower velocity in the wake of a turbine structure [14], from predators [15], or for enhanced foraging or attraction to the structure (a fish attracting device) [16].

The tidal-coupling observed at tidal stream sites occurs in parallel with diel-coupling (i.e., over a 24-h daily cycle); for example, the dispersal of herring and mackerel in low light [17,18] and diel vertical migration of herring [19] have been used to explain diel effects at other tidal sites [20,21].

As foraging efficiency controls both adult and juvenile survival and condition, changes in foraging efficiencies could have widespread effects on predator populations [22]. Hence, changes in the near and far field hydrodynamic conditions arising from the installation and operation of tidal turbines and the potential for changes to foraging efficiency need to be understood to predict the population level effects of turbine arrays [23].

### 1.3. Fish and tidal turbines

Fish behaviour has been studied in the context of tidal turbines ranging from presence [15,21,24,25] to vertical distribution [20,26] to behaviour and evasion [3,27–30], school morphology and predator-prey interactions [31]. However, concurrent physical parameters can be used to explain and predict the behaviours seen, allowing population-level and array-scale effects to be explored, and to predict predator behaviour. Fish passage rate in relation to tidal and diel phases has been explored in a high-velocity tidal channel, but without investigation of the effect of a turbine structure [21].

Increased fish abundance or increases in the predictability of fish behaviour around a turbine has the potential for both positive (e.g., predictable availability of prey) and negative (e.g., increasing collision risk) effects on predators. Conversely, decreased fish abundance may have a positive effect by decreasing collision risk of predators and prey with turbine blades, but also reduce foraging efficiency and displace predators from a site. Other studies (e.g., Ref. [21]) have considered individual fish passage rate; however, the focus of this study is the behaviour of fish schools as most predation takes place as foraging events within schools of fish [1]. The majority of fish biomass within this study site is proposed to be comprised of schooling species [32].

The objectives of this study are to investigate the following in a tidal site, across spring/neap, ebb/flood and diel cycles, including changes around a turbine structure:

1. The occurrence of fish schools.
2. The trends and predictability of school size, defined as observed cross-sectional area (CSA).
3. The trends and predictability of school height above the seabed.

Simultaneous collection of environmental parameters allows the possible causes of any changes in observed fish school occurrence or characteristics to be explored, and any behavioural effects inferred. This study investigates if differences in fish school characteristics (e.g., school occurrence, CSA or height) in a high energy tidal site can be predicted from spring/neap, ebb/flood and diel cycles, and if these characteristics change with or without the presence of a turbine support structure.

## 2. Methods

### 2.1. FLOWBEC platform

The *Flow, Water Column and Benthic Ecology 4-D* (FLOWBEC-4D) project investigated the environmental and ecological effects of installing and operating marine renewable energy devices. The FLOWBEC seabed platform was developed, which integrated multiple instruments to concurrently monitor the physical and ecological environment in marine energy sites [33]. Onboard batteries and data storage provided continuous recording of a 14-day spring/neap tidal cycle, and allowed measurements to be taken adjacent to marine energy structures and in areas free from such devices [31].

An Imagenex 837B Delta T multibeam echosounder (vertical swath aligned with the tidal flow) was synchronised with an upward facing Simrad EK60 multifrequency (38, 120, 200 kHz) scientific echosounder sampling once per second [31]. A SonTek/YSI ADVOcean 5 MHz Acoustic Doppler Velocimeter (ADV) was used to measure mean flow and turbulence at a sampling frequency of either 16 or 20 Hz, recording for 25-min bursts separated by five-minute intervals [14]. The ADV probe was mounted within the frame of the FLOWBEC platform, oriented upwards so that the sampling volume was approximately 0.85 m above the seabed. The probe was positioned to ensure that the flow through the sampling volume was unobstructed along the axis of tidal flow to minimise any interference from frame components as much as possible given practical limitations [14]. A WET Labs ECO FLNTUSB fluorometer measured chlorophyll-*a* concentration and turbidity. Field measurements were complemented with 15-min resolution outputs from a 3D hydrodynamic model with 20 depth layers and a cell size of 100 × 100 m at the FLOWBEC deployment locations, developed in Finite Volume Coastal Ocean Model (FVCOM) by FLOWBEC-4D project partners P. Cazenave and R. Torres at the Plymouth Marine Laboratory, U.K. [34].

### 2.2. Summary of deployments

This study focuses on two consecutive deployments of the FLOWBEC platform (2 Jun – 15 Jun 2013 and 18 Jun – 5 Jul 2013) at the European Marine Energy Centre (EMEC) Fall of Warness (FoW) tidal site in Orkney, Scotland (Fig. 1) [33], which provides seven grid-connected tidal turbine berths. A deployment 22 m from the centre of the Atlantis AK-1000 tidal turbine base (FoW1, Fig. 2) is compared to a "reference" deployment, in similar conditions 424 m away in an area free from devices (FoW2). The turbine support structure included a 10-m high piling, and three 4-m high ballast blocks; no nacelle or blades were present and there were no opportunities to deploy adjacent to an operational tidal turbine. For reference, the blades for the AK-1000 turbine were 18 m in diameter, with a rotor swept height of approximately 4.5–22.5 m above the seabed.

The two sites had comparable: depth of approximately 35 m; flow speeds up to 4 m/s; substrate and topography verified by remotely operated vehicle (ROV) surveys; distance from shore; and natural hydrodynamic conditions verified by hydrodynamic model outputs and ADV measurements [14,33]. This minimised the effects of natural spatial variations and maximised spatial comparability, such that any difference observed between the two sites could be attributed to the presence/absence of the turbine structure. Deployments were back-to-back to maximise temporal comparability and to minimise changes in fish abundance or the relative abundance of different species over the period of deployments.

### 2.3. Detecting fish schools

Fish schools were detected and discriminated from sources of interference, including backscatter relating to turbulence, using multifrequency EK60 data and the methods described in Fraser et al. [35]. This approach used adaptive processing to preserve sensitivity throughout the dynamic conditions, with multifrequency validation and manual inspection providing robust detection. A volume backscattering strength ($S_v$) threshold of −55 dB was applied to each sample, with a minimum 10-sample connected region to identify a fish school. The resolution of each sample (or pixel) was 0.19 m vertically, and 1 s horizontally determined by the EK60 sampling interval. Depth-mean flow velocity information (Fig. S2) was used to transform target persistence (time) into approximate target length.

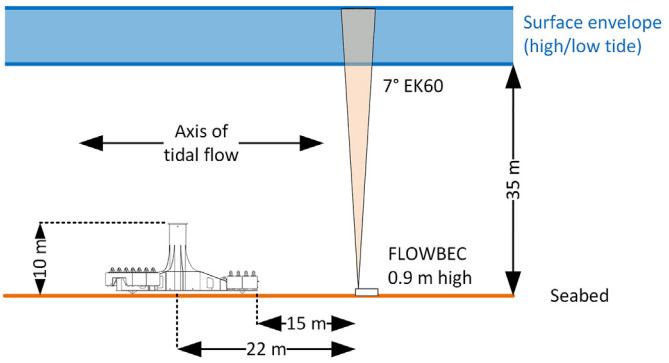


**Fig. 2.** The FoW1 deployment was downstream of the Atlantis turbine structure during flood flow, approximately 22 m from the centre of the 10-m high piling, and approximately 15 m from 4-m high ballast blocks; no nacelle or blades were present. Figure adapted from Williamson et al. [31].

Schools were delineated and recorded with their mean height above the seabed. This study used fish school observed cross-sectional area (CSA, unit $m^2$) as a measure of the size of a fish school. The calculation of CSA assumes that all schools are drifting passively with the depth-mean flow speed and does not account for swimming behaviour. Schools actively swimming with the tide will be underestimated in terms of CSA as they will move through the EK60 sampling volume more rapidly than if they were drifting with the depth-mean flow speed. Schools actively swimming against the tide or holding station will have their CSA overestimated as they remain in the EK60 sampling volume for longer. However, it is likely that all fish are swimming (or at least attempting to swim) against the current as that is the mode of highest energetic efficiency ([36] and references within) and therefore any CSA overestimate is systematically biased in the same direction, making comparison

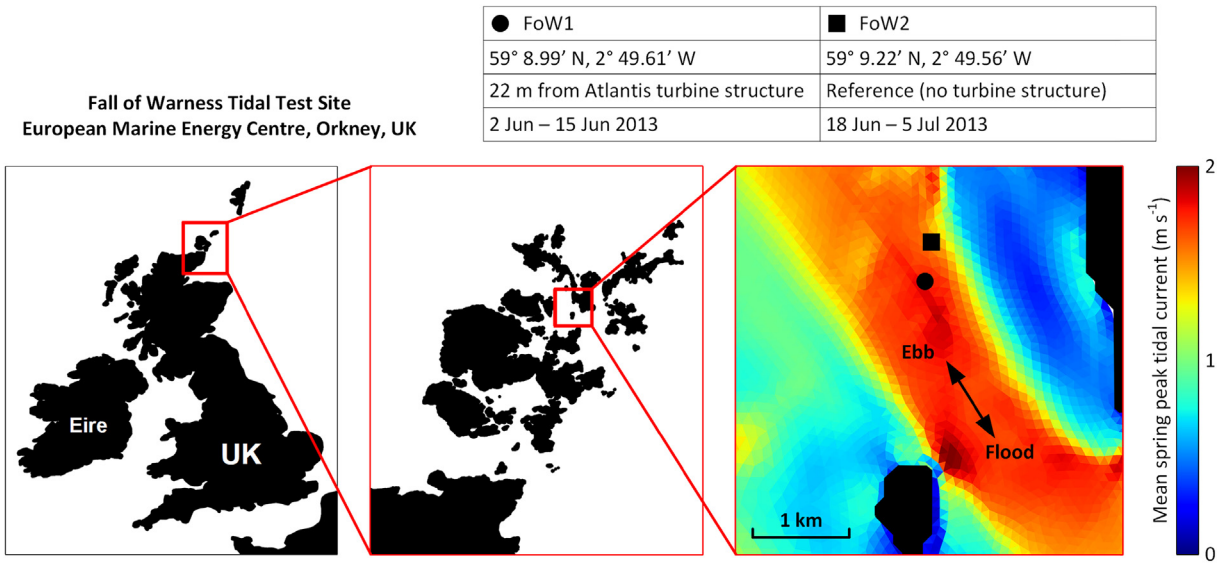


**Fig. 1.** Two deployments of the FLOWBEC platform are used to compare the predictability of fish school behavioural characteristics around a turbine structure (FoW1) and in the absence of a turbine structure (FoW2). Figure adapted from Williamson et al. [31]. The map shows the mean spring peak tidal current, which is the mean of a 12-h period surrounding peak spring flow from model outputs provided by FLOWBEC project partners P. Cazenave and R. Torres, Plymouth Marine Laboratory (U.K.) [34]. Peak spring tides reach 4 m/s.

between the values at different speeds meaningful.

CSA does not account for the density or the biomass of a school. The use of an acoustic density metric, such as mean volume backscattering strength ($S_v$), was calculated (Fig. S1) but was discounted in the absence of reliable species identification to avoid introducing an unknown species dependence into the results, i.e. the difference in target strength between fish with a swim bladder and those without. This study could not discriminate fish species as ground truthing trawls are not possible to conduct in such extreme high-energy tidal sites. However, other studies have suggested that fish species likely to be present in the Fall of Warness during the summer spawning season include Atlantic mackerel (*Scomber scombrus*), Atlantic herring (*Clupea harengus*), sprat (*Sprattus sprattus*), sand eel (*Ammodytes* sp.), haddock (*Melanogrammus aeglefinus*), ling (*Molva molva*), saithe (*Pollachius virens*), Atlantic cod (*Gadus morhua*), butterfish (*Pholis gunnellus*) and scorpion fish (*Taurulus bubalis*) [32]. Pollock (*Pollachius pollachius*) have been observed in visual data, with the observation that fish predominantly occur in aggregations rather than as individual fish [24]. Aggregations of gadoid fish were observed during ROV operations around the FLOWBEC platform and observations of sand eels and clupeid species have been seen in the bills of foraging birds in this site during surveys in 2012–13 [9,34].

### 2.4. Processing physical covariates as explanatory variables

Five physical covariates were processed as potential explanatory variables for fish school behaviour: time of day, depth-mean flow speed, depth-mean flow direction, flood/ebb index for timing relative to the minimum and maximum flow speed and direction, and spring/neap index for timing relative to variation in the range of tide height and flow speed over a 14-day cycle with the maximum range of tide height and flow speed occurring at spring tides. These physical covariates are defined as follows.

Time of day is a cyclic variable defined between 0 and 1 (midnight) with 0.5 corresponding to noon each day. Depth-mean flow speed and direction at the time of each fish school detection were linearly interpolated from 15-min interval 3D hydrodynamic model outputs [34] and vertically-averaged over the full water column. Model outputs were verified to be in phase with near-bed flow measurements from the ADV on the FLOWBEC platform which sampled at 16–20 Hz.

Flood/ebb index is a cyclic variable defined over each flood/ebb cycle based on flow speed rather than tide height due to a significant phase mismatch between tide height and speed at this site [9]. The lowest tide height occurs at the near-maximum flow speed, with near-zero speeds at approximately mid-height, and fast flowing tides at high water (Fig. S2, Supporting Information). Values of 0–0.5 represent the flood tidal flow (in a south-easterly direction) and values of 0.5–1 represent the ebb tidal flow (in a north-westerly direction). Values of 0/0.5/1 represent slack water. At the FoW1 site, the FLOWBEC platform is in the wake of the turbine structure during flood tides. The natural flow is largely bi-directional and symmetric at both FoW1 and FoW2 sites.

Spring/neap index is a cyclic variable defined between the points of highest water at each spring tide (0/1) with 0.5 corresponding to the highest water at the intervening neap tide. Tide height was measured by a pressure sensor on the FLOWBEC platform which sampled at 4 Hz.

### 2.5. Data analysis approaches

Differences in fish school vertical distributions are investigated for flow speeds above and below a nominal tidal turbine cut-in speed of 1 m/s [5]. The nonparametric two-sample Kolmogorov-Smirnov test was used to test for statistically significant differences between distributions using a significance level of $P < 0.05$. The modality of the probability density of distributions was estimated using Gaussian finite mixture models fitted via the expectation-maximisation algorithm using the mclust package [37] in R version 3.3.3 (R Development Core Team 2017). Mann-Whitney *U* tests were used to determine differences between the number of schools per hour and also the CSA of fish schools per hour in the presence and absence of a turbine structure. Generalised Additive Models (GAMs) using the mgcv package in R [38] were used to investigate which factors were influencing the distribution of school CSA and the height of schools (response variables).

Autocorrelation was investigated using Autocorrelation Function (ACF) plots (Fig. S3, Supporting Information). Autocorrelation was deemed not to be significant in the data, therefore mixed models incorporating correlation structures were not used.

A negative binomial distribution was used to model school CSA and a Gaussian distribution was used to model school height. These distributions were selected based on histograms of the data (Fig. S4, Supporting Information) and inspection of summary plots from the models (Figs. S5–S8, Supporting Information). A cyclic cubic regression spline was used to model time of day, depth-mean direction, flood/ebb index and spring/neap index. A thin plate regression spline was used to model depth-mean speed.

Generalised cross validation was used to choose the number of knots, and splines were inspected to ensure the models were not over-fitted.

Smoothing parameters were estimated using maximum likelihood. Model selection was performed using backwards selection based on P-values in which the least significant variable was removed until all variables were significant using a significance level of $P < 0.05$. The model selection is detailed in Table S1, Supporting Information. Different models were used to test the ability of the full range of explanatory variables to explain the variance in the CSA of schools and the height of schools in the water column. Results were compared between FoW1 (with the turbine structure present) and FoW2 (without a turbine structure) to investigate the effect of the turbine structure on these relationships.

## 3. Results

### 3.1. Fish school occurrence

The occurrence of fish schools significantly increased around the turbine structure compared to the natural flow conditions (Table 1), both when considering the rate of schools per hour (1.74 times more, $W = 61506$, $P < 0.0001$) and the mean observed school area per hour (1.75 times more, $W = 62495$, $P < 0.0001$).

#### 3.1.1. Flood/ebb differences

The increase in rate of schools per hour around the turbine structure was significant during the ebb tide (Fig. 3), i.e. when taking measurements upstream of the turbine structure (1.34 times more, $W = 14360.5$, $P = 0.0311$), and highly significant when taking measurements downstream of the turbine structure (2.17 times more, $W = 16304.5$, $P < 0.0001$). The natural flood-ebb symmetry in the absence of the turbine structure (mean flood rate 1.11 schools/hour, mean ebb rate 1.09 schools/hour) changes around the turbine structure (mean flood rate 2.41 schools/hour, mean ebb rate 1.45 schools/hour) with 1.66 times more schools downstream of the turbine structure (flood) than upstream of the turbine structure (ebb) ($W = 10801$, $P = 0.0257$).

#### 3.1.2. Diel effects

The increase in the rate of fish schools around the turbine

structure (Fig. 4) occurs in both the day (1.51 times more, $W = 34071$, $P < 0.0001$) and particularly the night (2.63 times more, $W = 3995$, $P = 0.0001$).

There is no significant difference between the number of schools observed during the day compared to the night in the natural flow conditions (1.18 times more in the day, $W = 12812$, $P = 0.4385$) or around the turbine structure (1.48 times more in the night, $W = 7818$, $P = 0.0802$).

Ebb (upstream) school occurrence is similar between the natural flow conditions and the turbine structure in the day (turbine structure 0.99 of the rate of the natural flow, $W = 5691$, $P = 0.4914$) but different at night (2.26 times higher rate around the turbine structure, $W = 868$, $P = 0.0091$). Flood (downstream) school occurrence is greater in the day (2.03 times more, $W = 5306$, $P < 0.0001$) and at night (2.75 times more, $W = 221$, $P = 0.0062$) when comparing measurements around the turbine structure to the natural flow conditions.

#### 3.1.3. Flow speed effects

In the natural flow conditions, the rate of schools observed above flow speeds of 1 m/s compared to those observed below 1 m/s is similar (1.48 times more, $W = 11303$, $P = 0.1493$). However, a significant difference occurs around the turbine structure with more schools seen below 1 m/s (2.02 times more, $W = 9302$, $P < 0.0001$), and this increase in school occurrence is concentrated during the flood (2.46 times more, $W = 2782$, $P < 0.0001$) rather than the ebb (1.19 times more, $W = 1744$, $P = 0.2320$) (see Fig. 3).

This increase in the occurrence of schools around the turbine structure compared to the natural flow conditions below flow speeds of 1 m/s in the ebb (upstream) is not significant (1.84 times more, $W = 466$, $P = 0.2570$) but is significant during the flood (downstream) (5.66 times more, $W = 408$, $P < 0.0001$). These differences between the two sites below flow speeds of 1 m/s are consistent across day (3.90 times more) and night (3.61 times more) (see Fig. 4).

### 3.2. Fish school CSA

The CSA of schools is driven by tidal and diel cycles at both sites (Fig. 5 rows 3–4, Table 2).

In natural flow conditions, the high numbers of schools occurring just before sunset (Fig. 5C) have a high area (Fig. 5F) and the schools with the highest area occur at high water (Fig. 5G), shortly before high slack water. School area has a minimum shortly after neap tides and a maximum shortly after spring tides.

The trends and predictability of school area change with the presence of the turbine structure. School area is still driven by diel cycles; however, the largest schools now occur shortly after midnight and midday in the presence of the turbine structure. The dependence of area on flow direction becomes significant. The largest schools occur at approximately high and low water, and the increase in the rate of school occurrence in the wake of the turbine structure at flow speeds below 1 m/s (Fig. 5A) is comprised of schools with a low area (Fig. 5E). The low number of schools at flow speeds above 1 m/s downstream of the turbine structure (Fig. 5B) is associated with schools with a high area (Fig. 5D).

### 3.3. Fish school height above the seabed

School height above the seabed is tidally-driven at both sites (Fig. 5 rows 5–6, Table 2).

In the natural flow conditions, the low (14.5%) deviance explained shows a relatively high variability. Vertical fish school distribution is similar between the ebb and flood for all schools ($P = 0.89$) (Fig. 3C&D), including for schools above ($P = 0.96$) and below ($P = 0.77$) a flow speed of 1 m/s. The vertical distribution of schools during the day (Fig. 4C) is tri-modal, suggesting different species exhibiting different behaviours. At night (Fig. 4D), schools were higher in the water column, with a significant difference ($P < 0.0001$) in distribution that becomes unimodal at night, suggesting all species are behaving in the same manner or that only one species is present during the night.

Trends and significant explanatory variables of school height change in the presence of the turbine structure, with school height becoming more predictable (27.7% deviance explained). School height is still tidally-driven, although with a single maximum of school height occurring at peak flood flow velocity, and a minimum of school height shortly before peak ebb flow velocity. The effect of flow speed now becomes significant at FoW1, with school height increasing with flow speed. A diel dependence now occurs, with

**Table 1**
FoW1 and FoW2 number of schools and school area, including rates per diel and tidal conditions using a reference speed of 1 m/s to represent a nominal turbine cut-in speed [26,31,35].

| | FoW1 (turbine structure) | FoW2 (natural conditions) |
|---|---|---|
| Number of schools | 523 | 396 |
| Sampling period (days) | 11.39 | 15.03 |
| Mean rate (schools/hour) | 1.91 | 1.10 |
| Mean observed school cross-sectional area per hour ($m^2$/h) | 24.17 | 13.80 |
| Mean day rate (schools/hour) | 1.72 | 1.14 |
| Mean day rate at flow speed < 1 m/s (schools/hour) | 2.73 | 0.70 |
| Mean day rate at flow speed ≥ 1 m/s (schools/hour) | 1.43 | 1.27 |
| Mean night rate (schools/hour) | 2.54 | 0.97 |
| Mean night rate at flow speed < 1 m/s (schools/hour) | 4.12 | 1.14 |
| Mean night rate at flow speed ≥ 1 m/s (schools/hour) | 1.88 | 1.00 |
| Mean rate at flow speed < 1 m/s (schools/hour) | 3.09 | 0.81 |
| Mean rate at flow speed ≥ 1 m/s (schools/hour) | 1.53 | 1.20 |
| Mean ebb rate (schools/hour) | 1.45 | 1.09 |
| Mean ebb rate at flow speed < 1 m/s (schools/hour) | 1.68 | 0.91 |
| Mean ebb rate at flow speed ≥ 1 m/s (schools/hour) | 1.41 | 1.19 |
| Mean flood rate (schools/hour) | 2.41 | 1.11 |
| Mean flood rate at flow speed < 1 m/s (schools/hour) | 4.13 | 0.73 |
| Mean flood rate at flow speed ≥ 1 m/s (schools/hour) | 1.68 | 1.20 |
| Mean day ebb rate (schools/hour) | 1.22 | 1.23 |
| Mean night ebb rate (schools/hour) | 2.08 | 0.92 |
| Mean day flood rate (schools/hour) | 2.09 | 1.03 |
| Mean night flood rate (schools/hour) | 3.58 | 1.28 |

minima in school height occurring at approximately midday and midnight. The vertical distribution of schools is altered around the turbine structure, with the mean school height now lower during the night than the day (Fig. 4A&B). The unimodal night-time distribution of fish in the absence of a turbine structure does not occur in the presence of the turbine structure, and the multimodal distribution more typical of daytime behaviour/presence occurs.

Differences in the vertical distribution between FoW1 and FoW2 are significant during the ebb ($P = 0.0006$) and flood ($P < 0.0001$). During the ebb (Fig. 3A), schools are absent below 5.5 m from the seabed at flow speeds above 1 m/s compared to FoW2 (Fig. 3C).

As well as increasing the number of schools, the turbine structure also causes a flood/ebb asymmetry in distribution (Fig. 3, $P = 0.02$) with a higher rate of occurrence 8–20 m above the seabed in the flood tide (Fig. 3B). The vertical distribution of schools below 1 m/s is significantly different between the FoW1 ebb and flood ($P = 0.02$) and between the FoW1 flood and FoW2 flood ($P < 0.0001$).

## 4. Discussion

### 4.1. Predictable changes in fish school characteristics over tidal and diel cycles

This study has shown that fish school occurrence, area and height above the seabed in a high-energy tidal site exhibit significant variation under episodic ebb/flood forcing and across the diel cycle. These school characteristics can be used to infer fish school

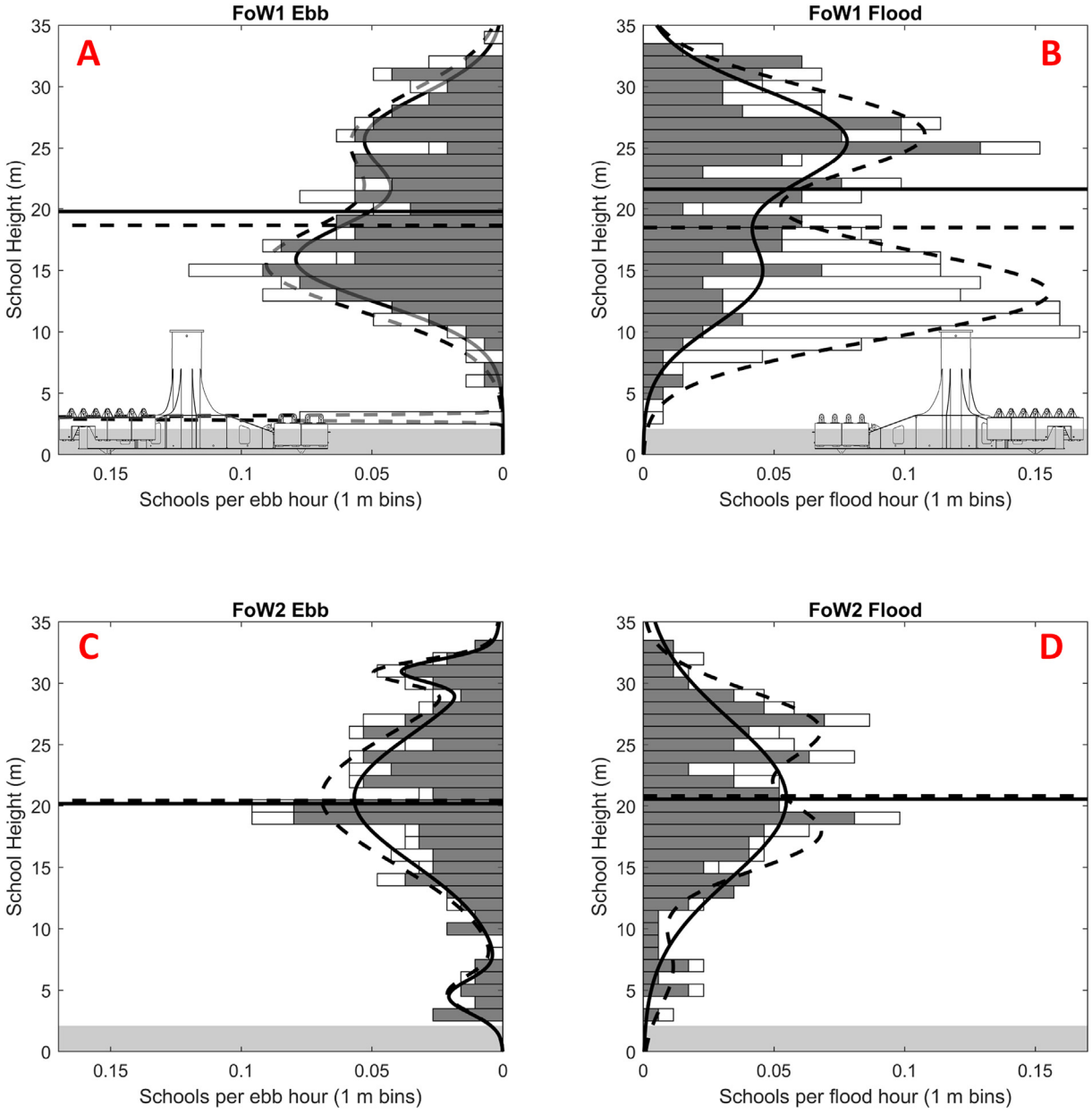


**Fig. 3.** Fish school vertical distribution across flood/ebb for all schools (open bars) with a mean height (dashed horizontal line) and for schools observed at flow speeds above a nominal turbine cut-in speed of 1 m/s (shaded bars) with a mean height (solid horizontal line). The lower extent of EK60 data processing is 2.1 m above the seabed (shaded area). A scaled representation of the turbine structure is shown at FoW1 (A and B). The probability densities of distributions estimated using Gaussian finite mixture models fitted via the expectation-maximisation algorithm are shown (curved solid line for schools at $\geq 1$ m/s and dashed curved line for all schools).

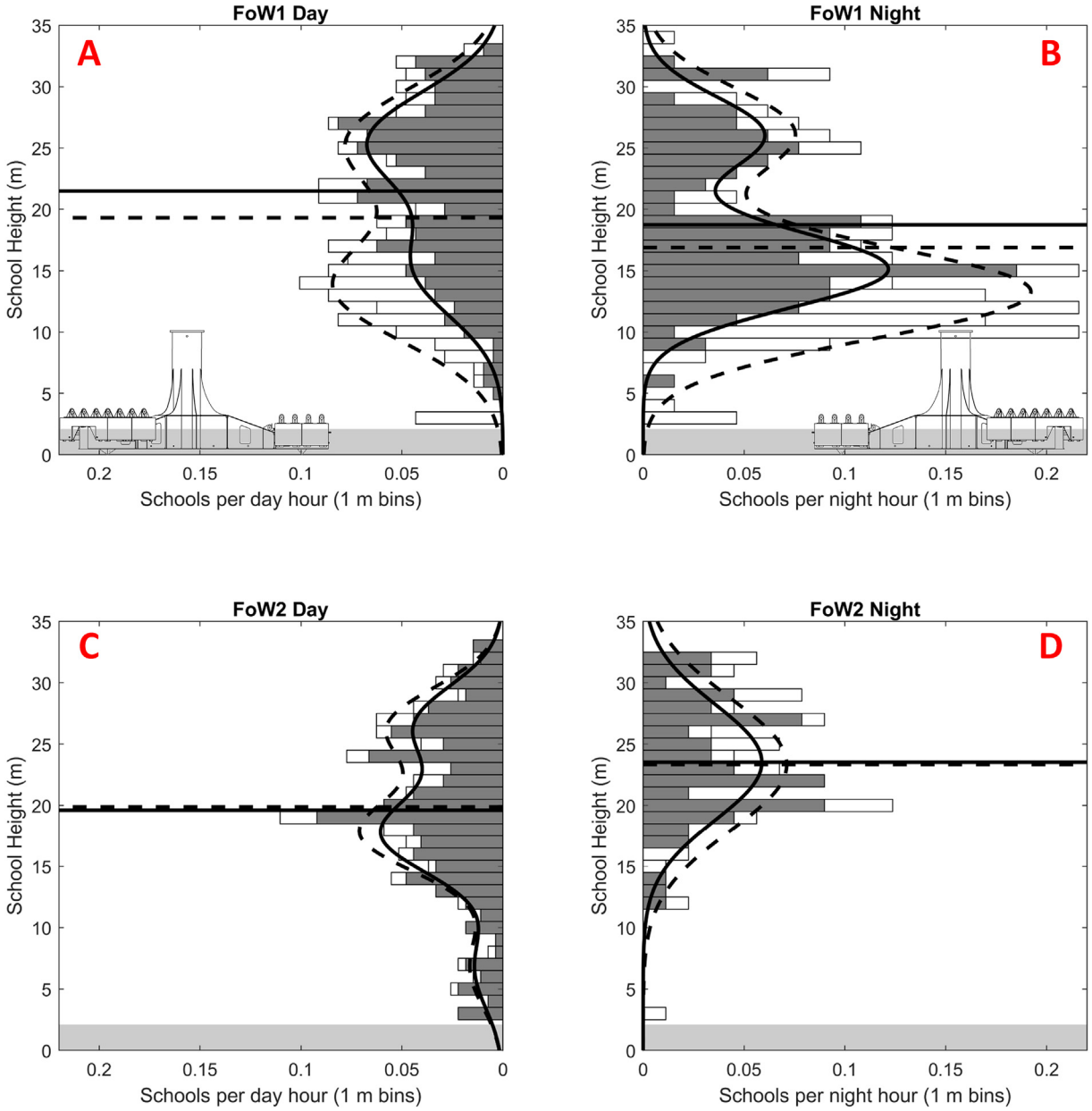


**Fig. 4.** Fish school vertical distribution across day/night for all schools (open bars) with a mean height (dashed horizontal line) and for schools observed at flow speeds above a nominal turbine cut-in speed of 1 m/s (shaded bars) with mean height (solid horizontal line). The lower extent of EK60 data processing is 2.1 m above the seabed (shaded area). A scaled representation of the turbine structure is shown at FoW1 (A and B). The probability densities of distributions estimated using Gaussian finite mixture models fitted via the expectation-maximisation algorithm are shown (curved solid line for schools at $\geq$ 1 m/s and dashed curved line for all schools).

behaviour when combined with environmental parameters. Concurrent ecological and physical measurements were used to reveal links between fish school characteristics and hydrodynamics, establishing the predictability of these characteristics over tidal and diel cycles.

This supports the theory of tidal coupling [8] and tidal forcing when flows exceed physiological limits [11] driving fish behaviour in tidal sites. Although this study observed diel trends in the vertical distribution of schools rather than direct observations of diel vertical migration, it is proposed that the tidal coupling/forcing is occurring in conjunction with diel effects comprising either diel vertical migration [17–19] or the presence of different species assemblages at different heights during the diel cycle.

Diel and tidal coupling were observed in other sites using a comparable metric of individual fish passage rate [21]. Although school CSA increased with increasing flow speed (Fig. 5), the rate of school occurrence per hour did not vary across flood/ebb index in the natural flow conditions (Fig. 5), similar to that seen at other tidal energy sites [21].

### 4.2. Changes in fish school characteristics around a turbine structure

The measured fish school characteristics (occurrence, area, height) changed with the presence of a non-operational turbine structure. A site with a turbine structure present was compared to a reference site with similar environmental conditions. Simultaneous reference measurements were not possible due to the logistical

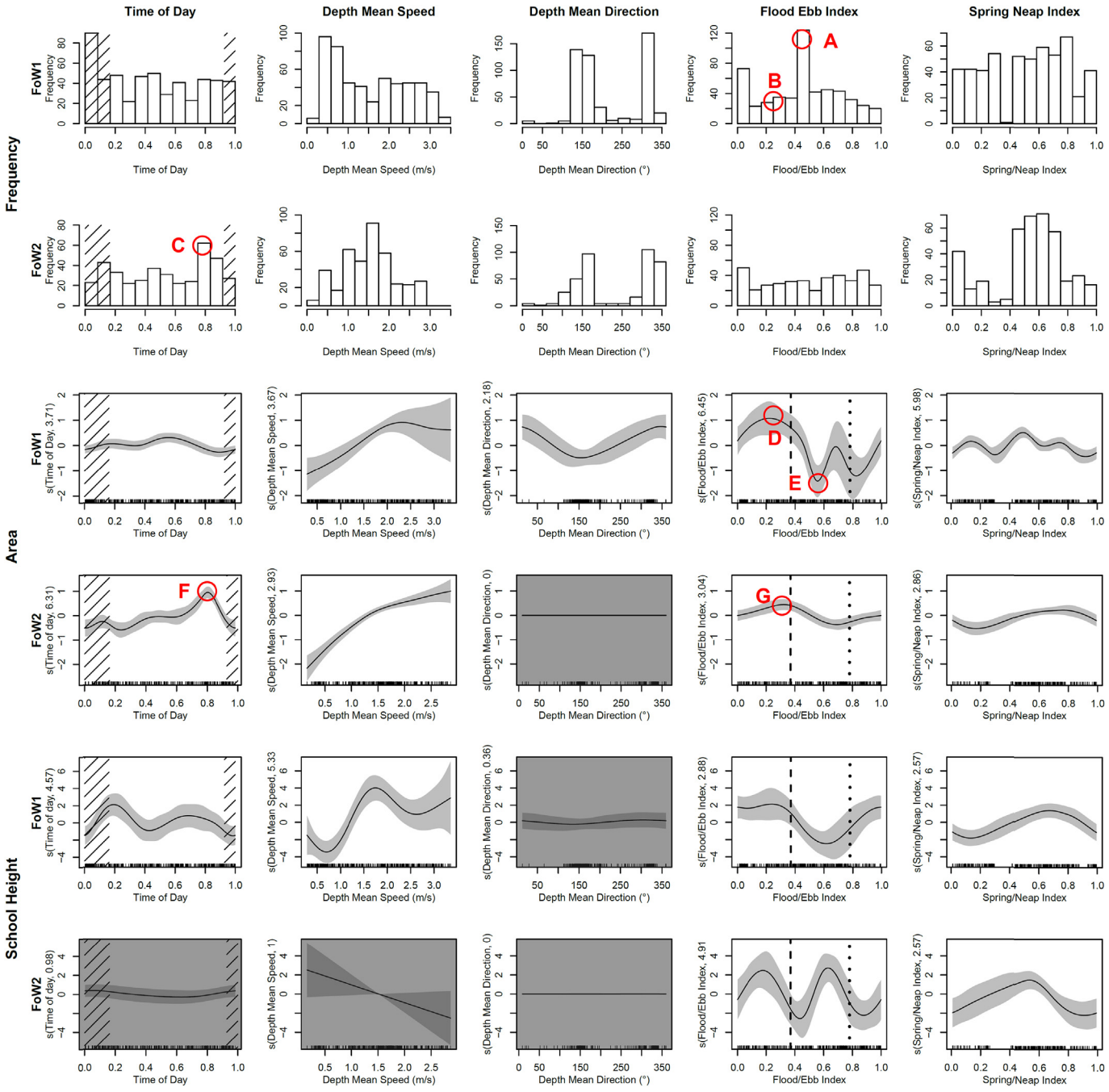


**Fig. 5.** Histograms show the frequency of schools for each covariate. GAM relationships (smoothing spline ± 2 SE) for school area and school height are shown. Greyed-out plots are non-significant. Y-axis labels show the estimated degrees of freedom. Periods of night are indicated (diagonal-hashed lines) on the time of day index. High (dashed) and low (dotted) water are indicated on the flood/ebb index. Labels A-G are considered in the text in section 3.2.

constraint of a single instrument platform; however, deployments were back-to-back in time to maximise comparability.

As well as changes in school characteristics around a turbine structure, there were significant differences above and below the flow speed at which a turbine would start operation. The presence of the turbine structure changed which environmental parameters were significant explanatory variables of the fish school behavioural characteristics. Tide direction became a significant explanatory variable of school CSA around the turbine structure, linked to the predictable occurrence of small schools downstream of the turbine structure. The turbine structure added a diel dependence to vertical distribution, which is of relevance to visual detection of an operational turbine in terms of collision risk, and to fish attraction as suggested elsewhere [15,24]. Changes to fish behaviour around the turbine structure support theories of refuge from predators [15], flow refuge [2], enhanced foraging opportunities or attraction to structures [16].

As these changes in school characteristics occurred across both diel and tidal cycles with observable effects in the wake and upstream of the turbine structure, it is hypothesised that the effects are caused by a combination of visual and hydrodynamic perception of the turbine structure. Concurrent ADV measurements of

**Table 2**
Variables included in the best models identified using GAMs with a significance level of $P < 0.05$. The estimated degrees of freedom (EDF) for the smoothed terms, chi-squared ($\chi^2$), F-test (F), P-values (P) and non-significant variables (NS) are shown.

| Location | Response variables | Explanatory variables | | | | | Deviance explained (%) | Number of schools |
|---|---|---|---|---|---|---|---|---|
| | | Time of day | Depth mean speed | Depth mean direction | Flood/ebb index | Spring/neap index | | |
| FoW1 | **School area** | EDF = 3.712<br>$X^2 = 17.202$<br>$P < 0.0001$ | EDF = 3.669<br>$X^2 = 40.315$<br>$P < 0.0001$ | EDF = 2.177<br>$X^2 = 11.622$<br>$P < 0.0001$ | EDF = 6.454<br>$X^2 = 44.236$<br>$P < 0.0001$ | EDF = 5.983<br>$X^2 = 36.479$<br>$P < 0.0001$ | 58.5 | 523 |
| FoW2 | **School area** | EDF = 6.309<br>$X^2 = 81.087$<br>$P < 0.0001$ | EDF = 2.931<br>$X^2 = 100.924$<br>$P < 0.0001$ | NS | EDF = 3.045<br>$X^2 = 23.540$<br>$P < 0.0001$ | EDF = 2.858<br>$X^2 = 19.785$<br>$P < 0.0001$ | 54.4 | 396 |
| FoW1 | **School height** | EDF = 4.579<br>F = 1.911<br>P = 0.0032 | EDF = 5.379<br>F = 8.355<br>$P < 0.0001$ | NS | EDF = 2.819<br>F = 2.520<br>$P < 0.0001$ | EDF = 2.571<br>F = 2.436<br>$P < 0.0001$ | 27.7 | 523 |
| FoW2 | **School height** | NS | NS | NS | EDF = 5.274<br>F = 4.006<br>$P < 0.0001$ | EDF = 3.032<br>F = 3.911<br>$P < 0.0001$ | 14.5 | 396 |

mean velocity and turbulence characteristics in the near-bed environment have shown that hydrodynamic modification from the turbine structure is clearly detectable at the range at which fish school measurements were gathered; Fraser et al. [14] showed a 31% near-bed velocity deficit associated with comparatively high velocity fluctuations and enhanced turbulence in the wake of the turbine structure at this range. Ongoing work is investigating the incorporation of turbulence metrics into the predictive models. These turbulence metrics can be derived from measurements in the near-bed environment using the ADV, Acoustic Doppler Current Profiler (ADCP) data collected during subsequent deployments of the platform, and EK60 measurements of backscatter related to turbulence activity in the water column [35].

Significantly more schools per hour and a higher school area per hour around the turbine structure compared to the reference site were observed. An aggregating or attraction effect around an operational turbine has been observed in the Fall of Warness via camera observations [24] but only at low flow speeds. The changes in fish abundance were not evaluated through comparison to a site without a turbine and observations only took place visually during periods of good visibility (daylight and slower tidal speeds). This fish attracting effect of tidal turbine structures has been hypothesised, for example for refuge from predators or flow [15]. The opposite of an attracting effect was observed by Bevelhimer et al. [29] in a much smaller-scale site, where fish density was twice as high when a turbine was absent compared to operational. Avoidance by individual fish up to 140 m from a turbine was observed by Shen et al. [29], with far field avoidance also seen by Bevelhimer et al. [29]. The differences in these other studies may arise from device/site/species dependence, with Shen et al. [7] studying a horizontal axis turbine in Maine, and Bevelhimer et al. [29] studying a smaller 5-m diameter turbine in New York, in a site that is 240 m wide, 10 m deep with flows of up to 2.5 m/s.

### 4.3. Parameterisation of fish schools

It was proposed that the majority of fish biomass in the Fall of Warness is comprised of schooling species [32] and that predators are targeting schools of fish [1]. Therefore, the focus of this study was on schools, enabled by robust methods for fish school detection and discrimination from sources of interference, including backscatter relating to turbulence [35]. The filtering process excluded 2.4% of data such that any potential effect on target results is limited and a substantial improvement in data coverage compared with many existing approaches [35].

Fish school observed CSA was selected as the most appropriate measure of the size of a fish school as the absence of reliable species identification did not allow the use of an acoustic density metric such as mean volume backscattering strength ($S_v$). However, we compared the use of acoustic density metrics (Fig. S1) with CSA and found that the significant environmental predictor variables are similar, and yield similar trends. Further development of species classification will allow differences in fish species behaviour and their school density or biomass to be investigated in detail in the future. The calculation of CSA assumes that all schools are drifting passively with the depth-mean flow speed and does not account for swimming behaviour. This effect may be able to be corrected for by direct measurement of the swim speed of each fish school using co-registration of schools with the multibeam echosounder on the FLOWBEC platform [31] and forms the subject of ongoing work.

Should predators be targeting prey *aggregations* then the size of fish schools is important, i.e. if predators are targeting large schools because they are either easier to catch or have greater energetic benefits, then the presence, size and predictability of these large schools is important. However, if predators are targeting prey *availability* (the ease at which prey can be captured) then the number of schools is more important rather than the size of these schools [39], i.e. small schools will still be targeted if easy to catch [40]. Both effects may be (prey) species-dependent. Investigation of whether predators are targeting prey aggregations and/or availability is a focus of ongoing work using prey data from the FLOWBEC platform and vessel hydroacoustic surveys, combined with simultaneous predator observations from shore based observations over the FLOWBEC platform or from the vessel based surveys.

### 4.4. Potential additional effects of a turbine nacelle and blades

The 10-m high piling and 4-m high ballast blocks of the turbine structure in this study have been shown to change fish school occurrence and characteristics throughout the water column at a range of 15–22 m in this study. The techniques developed are directly applicable to an operational tidal turbine to investigate any additional effect of the nacelle and blades, and to investigate the predictability of fish behaviour and biophysical coupling to be tested at other sites. Measurements around an operating tidal turbine will inform whether any additional response to the rotating blades occurs, through either visual, hydrodynamic or acoustic detection, or their combination. At a smaller scale (5-m diameter turbine), Bevelhimer et al. [29] found significant differences in fish behaviour between turbine presence and operation, comprising small differences to swimming direction and velocity usually to avoid the rotating blades.

Horizontal (rather than vertical) avoidance of a horizontal-axis turbine at horizontal ranges of 10–140 m has been observed

elsewhere [7], but weak or no relationship was noted when the turbine was static, suggesting noise or visual cues were triggering a behavioural response rather than hydrodynamic stimuli [3]. This contrasts to the results of this study, which showed significant effects on fish school occurrence and characteristics even without the nacelle or rotating blades, with changes likely arising from the wake and structure (visual and hydrodynamic perception).

### 4.5. Management implications for collision risk and foraging efficiency

The mechanisms driving fish behavioural changes around turbine structures have implications for prey and predator collision risk with turbine blades [2], for example due to visibility affecting the perception of turbines, and flow speed determining turbine rotational speed and the reaction time needed to execute a successful evasion. The vertical distribution, schooling behaviour and attraction of fish schools to a turbine structure can be used as empirical data for collision risk modelling. Periods and locations of increased collision risk can be identified, and if necessary, selected for additional monitoring or mitigation. Grippo et al. [3] state that behavioural risk can be assumed to be minimal if the observed fish movement patterns suggest the turbine has only small and temporary effects on normal swimming patterns or fish distribution within a channel. However, predictable and consistent changes to prey distribution and behaviour will affect predator behaviour with implications for collision risk. For example, if predators are found to utilise periods of high flow velocity and hold station against the flow [10,41] while foraging around tidal turbines, then this will substantially increase predator collision risk by increasing the occurrences and duration of time the predator potentially spends in the rotor swept area.

The presence of fish lower in the water column at night around a turbine structure, within the anticipated rotor swept area, may have wider changes in energetics and collision risk such that they have effects at a population level. If the same change in behaviour occurs around an operational turbine, then predator and prey collision risk will increase due to a greater proportion of time spent in the rotor swept area. Similarly, there will be an increased chance of animals encountering moving blades during periods of reduced visual detectability at low light, should detection from flow field modification or noise not be sufficient to trigger an evasion response.

If predators are targeting the largest fish schools which occur at peak flow speeds whether a turbine structure is present or not, then there is no reason to suggest there is increased foraging due to turbine structures at these points in time. However, foraging at peak flow speeds will increase predator collision risk, as the turbine will be rotating. Conversely, if predators are targeting high numbers of schools, then predators will focus foraging on areas with turbine structures, and the predictable occurrence of schools downstream of the turbine structure irrespective of day or night may increase foraging efficiency. However, the high numbers of schools with a smaller CSA which predictably occur downstream of the turbine structure occur at flow speeds below 1 m/s when the turbine will not be rotating, as observed elsewhere [24], and thus there will not be a risk of predator collision with moving blades. However, it is worth keeping in mind that the different behaviours could be due to different fish species, and thus be targeted by differing predator foraging strategies.

The findings of this study have implications for changes to predator foraging efficiency arising from the installation of subsea structures [4]. Hydrodynamic patterns associated with the tidal flow [1], and hydrodynamic modifications from the turbine structure [14] have been hypothesised to aggregate, disaggregate and disorient prey, causing changes in prey availability and foraging efficiency [23,34] affecting energetics at both individual levels and possibly sufficient to affect population levels. This understanding of the physical and ecological effects of the turbine structure, and the predictability of fish behaviour around the turbine structure will inform the monitoring and management of operating tidal turbines. With a greater understanding of how and why mobile predators use specific biophysical conditions in high-energy areas for foraging, the predictive power of the outcomes may lead to a wider strategic approach to monitoring and a reduction in the level of monitoring required to support the sustainable development of tidal energy.

## Declarations of interest

None.

## Acknowledgements

We acknowledge the support of Philippe Blondel, Paul Bell, James Waggitt, Ian Davies, Eric Armstrong, staff at Marine Scotland Science and the European Marine Energy Centre. Hydrodynamic model data were provided by P. Cazenave and R. Torres (Plymouth Marine Laboratory). The constructive comments from the reviewers of earlier versions of this manuscript are gratefully acknowledged.

## Appendix A. Supplementary data

Supplementary data to this article can be found online at https://doi.org/10.1016/j.renene.2019.04.065.

## Funding

This work was funded by NERC and Defra (NE/J004308/1, NE/J004200/1 and NE/J004332/1). BW was also funded by a NERC MREKEP Internship, an Innovate UK KTP with MeyGen Ltd. (KTP009812), the NERC VertIBase project (NE/N01765X/1) and the UK Department for Business, Energy and Industrial Strategy's offshore energy Strategic Environmental Assessment programme.

## References

[1] S. Benjamins, A.C. Dale, G.D. Hastie, J.J. Waggitt, M. Lea, B.E. Scott, B. Wilson, Confusion reigns? A review of marine megafauna interactions with tidal-stream environments, Oceanogr. Mar. Biol. (2015) 1–54, https://doi.org/10.1201/b18733-2.

[2] A. Copping, N. Sather, L. Hanna, J. Whiting, G. Zydlewski, G. Staines, A. Gill, I. Hutchison, A. O'Hagan, T. Simas, J. Bald, C. Sparling, J. Wood, E. Masden, Annex IV 2016 State of the Science Report: Environmental Effects of Marine Renewable Energy Development Around the World, 2016. http://tethys.pnnl.gov/publications/state-of-the-science-2016.

[3] M. Grippo, H. Shen, G. Zydlewski, S. Rao, A. Goodwin, Behavioral Responses of Fish to a Current-Based Hydrokinetic Turbine under Multiple Operational Conditions, 2017, https://doi.org/10.2172/1348394. Final Report.

[4] D.J.F. Russell, S.M.J.M. Brasseur, D. Thompson, G.D. Hastie, V.M. Janik, G. Aarts, B.T. McClintock, J. Matthiopoulos, S.E.W. Moss, B. McConnell, Marine mammals trace anthropogenic structures at sea, Curr. Biol. 24 (2014) R638–R639, https://doi.org/10.1016/j.cub.2014.06.033.

[5] S. Baston, S. Waldman, J. Side, Modelling Energy Extraction in Tidal Flows, MASTS Position Paper, 2015, https://doi.org/10.13140/RG.2.1.4620.2481.

[6] L. Hammar, L. Eggertsen, S. Andersson, J. Ehnberg, R. Arvidsson, M. Gullström, S. Molander, A probabilistic model for hydrokinetic turbine collision risks: exploring impacts on fish, PLoS One 10 (2015), https://doi.org/10.1371/journal.pone.0117756.

[7] H. Shen, G.B. Zydlewski, H.A. Viehman, G. Staines, Estimating the probability of fish encountering a marine hydrokinetic device, Renew. Energy 97 (2016) 746–756, https://doi.org/10.1016/j.renene.2016.06.026.

[8] J.E. Zamon, Mixed species aggregations feeding upon herring and sandlance schools in a nearshore archipelago depend on flooding tidal currents, Mar. Ecol. Prog. Ser. 261 (2003) 243–255, https://doi.org/10.3354/meps261243.

[9] J.J. Waggitt, P. Cazenave, R. Torres, B.J. Williamson, B.E. Scott, Quantifying pursuit diving seabirds' associations with fine-scale physical features in tidal stream environments, J. Appl. Ecol. 23 (2016) 1653–1666, https://doi.org/10.1111/1365-2664.12646.
[10] G.D. Hastie, D.J.F. Russell, S. Benjamins, S. Moss, B. Wilson, D. Thompson, Dynamic habitat corridors for marine predators; intensive use of a coastal channel by harbour seals is modulated by tidal currents, Behav. Ecol. Sociobiol. 70 (2016) 2161–2174, https://doi.org/10.1007/s00265-016-2219-7.
[11] J.J. Videler, F. Hess, Fast continuous swimming of two pelagic predators, saithe (Pollachius virens) and mackerel (Scomber scombrus): a kinematic analysis, J. Exp. Biol. 109 (1984) 209 LP–228.
[12] T. O'Doherty, A. Mason-Jones, D.M. O'Doherty, P.S. Evans, C. Wooldridge, I. Fryett, Considerations of a horizontal axis tidal turbine, Proc. Inst. Civ. Eng. Energy 163 (2010) 119–130, https://doi.org/10.1680/ener.2010.163.3.119.
[13] T. Stallard, R. Collings, T. Feng, J. Whelan, Interactions between tidal turbine wakes: experimental study of a group of three-bladed rotors, Philos. Trans. R. Soc. A Math. Phys. Eng. Sci. 371 (2013), https://doi.org/10.1098/rsta.2012.0159.
[14] S. Fraser, V. Nikora, B.J. Williamson, B.E. Scott, Hydrodynamic impacts of a marine renewable energy installation on the benthic boundary layer in a tidal channel, Energy Procedia 125 (2017) 250–259, https://doi.org/10.1016/j.egypro.2017.08.169.
[15] S.H. Kramer, C.D. Hamilton, G.C. Spencer, H.O. Ogston, Evaluating the Potential for Marine and Hydrokinetic Devices to Act as Artificial Reefs or Fish Aggregating Devices, Based on Analysis of Surrogates in Tropical, Subtropical, and Temperate US West Coast and Hawaiian Coastal Waters, HT Harvey & Associates, Honolulu, HI (United States), 2015, https://doi.org/10.2172/1179455.
[16] G.W. Boehlert, A.B. Gill, Environmental and ecological effects of ocean renewable energy development: a current synthesis, Oceanography 23 (2010) 68–81, https://doi.org/10.5670/oceanog.2010.46.
[17] J.H.S. Blaxter, R.S. Batty, Herring behaviour in the dark: responses to stationary and continuously vibrating obstacles, J. Mar. Biol. Assoc. U. K. 65 (1985) 1031–1049, https://doi.org/10.1017/S0025315400019494.
[18] C.W. Glass, C.S. Wardle, W.R. Mojsiewicz, A light intensity threshold for schooling in the Atlantic mackerel, Scomber scombrus, J. Fish Biol. 29 (1986) 71–81, https://doi.org/10.1111/j.1095-8649.1986.tb05000.x.
[19] L. Nilsson, U.H. Thygesen, B. Lundgren, B.F. Nielsen, J.R. Nielsen, J.E. Beyer, Vertical migration and dispersion of sprat *(Sprattus sprattus)* and herring *(Clupea harengus)* schools at dusk in the Baltic Sea, Aquat. Living Resour. 16 (2003) 317–324, https://doi.org/10.1016/S0990-7440(03)00039-1.
[20] H.A. Viehman, G.B. Zydlewski, J.D. McCleave, G.J. Staines, Using hydroacoustics to understand fish presence and vertical distribution in a tidally dynamic region targeted for energy extraction, Estuar. Coasts (2014), https://doi.org/10.1007/s12237-014-9776-7.
[21] H.A. Viehman, G.B. Zydlewski, Multi-scale temporal patterns in fish presence in a high-velocity tidal channel, PLoS One (2017), https://doi.org/10.1371/journal.pone.0176405.
[22] M. Begon, C.R.H. Townsend, L. John, R.T. Colin, L.H. John, Ecology: from Individuals to Ecosystems, 2006.
[23] B.E. Scott, R. Langton, E. Philpott, J.J. Waggitt, Seabirds and marine renewables: are we asking the right questions? in: M.A. Shields, A.I.L. Payne (Eds.), Mar. Renew. Energy Technol. Environ. Interact. Springer Netherlands, 2014, pp. 81–92, https://doi.org/10.1007/978-94-017-8002-5_7.
[24] M. Broadhurst, S. Barr, C.D.L. Orme, In-situ ecological interactions with a deployed tidal energy device; an observational pilot study, Ocean Coast Manag. 99 (2014) 31–38, https://doi.org/10.1016/j.ocecoaman.2014.06.008.
[25] L. Hammar, S. Andersson, L. Eggertsen, J. Haglund, M. Gullström, J. Ehnberg, S. Molander, Hydrokinetic turbine effects on fish swimming behaviour, PLoS One 8 (2013), e84141, https://doi.org/10.1371/journal.pone.0084141.
[26] S. Fraser, B.J. Williamson, V. Nikora, B.E. Scott, Fish distributions in a tidal channel indicate the behavioural impact of a marine renewable energy installation, Energy Rep. 4 (2018) 65–69, https://doi.org/10.1016/j.egyr.2018.01.008.
[27] H.A. Viehman, G.B. Zydlewski, Fish interactions with a commercial-scale tidal energy device in the natural environment, Estuar. Coasts 38 (2015) 241–252, https://doi.org/10.1007/s12237-014-9767-8.
[28] S.V. Amaral, M.S. Bevelhimer, G.F. Čada, D.J. Giza, P.T. Jacobson, B.J. McMahon, B.M. Pracheil, Evaluation of behavior and survival of fish exposed to an axial-flow hydrokinetic turbine, N. Am. J. Fish. Manag. 35 (2015) 97–113, https://doi.org/10.1080/02755947.2014.982333.
[29] M. Bevelhimer, C. Scherelis, J. Colby, M.A. Adonizio, Hydroacoustic assessment of behavioral responses by fish passing near an operating tidal turbine in the east river, New York, Trans. Am. Fish. Soc. 146 (2017) 1028–1042, https://doi.org/10.1080/00028487.2017.1339637.
[30] M. Bevelhimer, J. Colby, M.A. Adonizio, C. Tomichek, C. Scherelis, Informing a Tidal Turbine Strike Probability Model through Characterization of Fish Behavioral Response Using Multibeam Sonar Output, Oak Ridge National Laboratory (ORNL), Oak Ridge, TN (United States), 2016, https://doi.org/10.2172/1324172.
[31] B.J. Williamson, S. Fraser, P. Blondel, P.S. Bell, J.J. Waggitt, B.E. Scott, Multisensor acoustic tracking of fish and seabird behavior around tidal turbine structures in Scotland, IEEE J. Ocean. Eng. 42 (2017), https://doi.org/10.1109/JOE.2016.2637179.
[32] AURORA Environmental Ltd, Environmental Statement, EMEC Tidal Test Facility Fall of Warness REP143-01-02, 2005. http://www.emec.org.uk/?wpfb_dl=54.
[33] B.J. Williamson, P. Blondel, E. Armstrong, P.S. Bell, C. Hall, J.J. Waggitt, B.E. Scott, A self-contained subsea platform for acoustic monitoring of the environment around marine renewable energy devices – field deployments at wave and tidal energy sites in Orkney, Scotland, IEEE J. Ocean. Eng. 41 (2016) 67–81, https://doi.org/10.1109/JOE.2015.2410851.
[34] J.J. Waggitt, P.W. Cazenave, R. Torres, B.J. Williamson, B.E. Scott, Predictable hydrodynamic conditions explain temporal variations in the density of benthic foraging seabirds in a tidal stream environment, ICES J. Mar. Sci. J. Du Cons. 73 (2016), https://doi.org/10.1093/icesjms/fsw100.
[35] S. Fraser, V. Nikora, B.J. Williamson, B.E. Scott, Automatic active acoustic target detection in turbulent aquatic environments, Limnol Oceanogr. Methods 15 (2017) 184–199, https://doi.org/10.1002/lom3.10155.
[36] C. Eloy, On the best design for undulatory swimming, J. Fluid Mech. 717 (2013) 48–89, https://doi.org/10.1017/jfm.2012.561.
[37] C. Fraley, A.E. Raftery, T.B. Murphy, L. Scrucca, Mclust Version 4 for R: Normal Mixture Modeling for Model-Based Clustering, Classification, and Density Estimation, 2012.
[38] S.N. Wood, Fast stable restricted maximum likelihood and marginal likelihood estimation of semiparametric generalized linear models, J. R. Stat. Ser. Soc. B Stat. Methodol. 73 (2011) 3–36, https://doi.org/10.1111/j.1467-9868.2010.00749.x.
[39] B.E. Scott, A. Webb, M.R. Palmer, C.B. Embling, J. Sharples, Fine scale biophysical oceanographic characteristics predict the foraging occurrence of contrasting seabird species; Gannet (*Morus bassanus*) and storm petrel (*Hydrobates pelagicus*), Prog. Oceanogr. 117 (2013) 118–129, https://doi.org/10.1016/j.pocean.2013.06.011.
[40] M. Chimienti, K.A. Bartoń, B.E. Scott, J.M.J. Travis, Modelling foraging movements of diving predators: a theoretical study exploring the effect of heterogeneous landscapes on foraging efficiency, PeerJ. 2 (2014) e544, https://doi.org/10.7717/peerj.544.
[41] H.M. Wade, E.A. Masden, A.C. Jackson, R.W. Furness, Which seabird species use high-velocity current flow environments? Investigating the potential effects of tidal-stream renewable energy developments, in: BOU Mar. Renewables Birds, 2012, https://doi.org/10.13140/2.1.2530.6885.